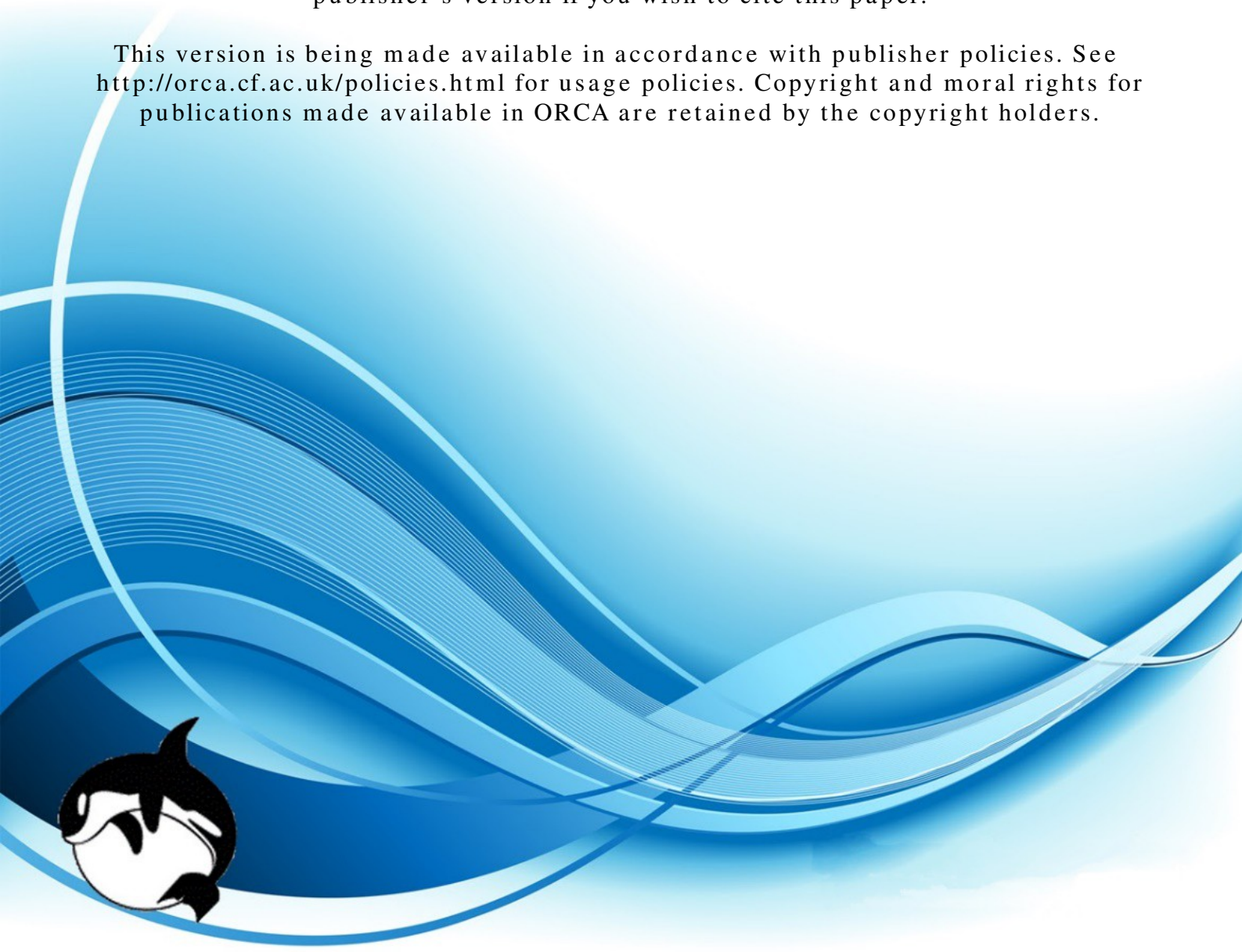

Simulation of the flow of self-compacting concrete in the V-funnel by SPH

W. S. Alyhya[1], S. Kulasegaram, B. L. Karihaloo[2]

School of Engineering

Cardiff University

CF24 3AA, UK

[1] On leave from college of Engineering, Kerbala University, Iraq

[2] Corresponding author (E-mail address: KarihalooB@Cardiff.ac.uk)

Abstract

The flow of self-compacting concrete (SCC) mixes through a V-funnel is simulated from the moment the gate is opened until the time when the light was first seen in the bottom opening through observation from the top (discharge time, $t_{v\text{-}funnel}$). For this simulation, the three-dimensional mesh-less smooth particle hydrodynamics (SPH) computational approach is chosen in which the SCC mix is treated as a non-Newtonian Bingham-type fluid. The numerical simulation results for the discharge time agree very favourably with those recorded in the laboratory on a range of normal strength SCC mixes with cube compressive strengths from 30 to 80 MPa with a maximum size crushed coarse aggregate of 20 mm. In contrast, the two-dimensional simulation of the V-funnel test is found to underestimate significantly the discharge time. The statistics of the distribution of the coarse aggregate particles equal to or larger than 8 mm in the mix (this limit is set by the number of particles used in the SPH simulations) shows that the mix remains homogeneous with no settlement of the heavier particles during the flow and after the flow has stopped.

Keywords: Self-compacting concrete; V-funnel; 3D simulation; SPH; Bingham parameters

1. Introduction

In concrete construction, insufficient filling of formwork and de-airing and segregation of conventional vibrated mix components give rise to serious durability problems. The impact of such problems has increased sharply as complex formwork and/or dense reinforcement is being used. Self-compacting concrete (SCC) which flows and consolidates under the action of gravity, without external vibration, while maintaining homogeneity has been developed to overcome these problems [1]. It ensures proper filling of formwork and produces a high quality finish in heavily reinforced structural members and inaccessible areas even in the most complex formwork.

Various tests are performed to evaluate the fresh properties of SCC, including its filling ability, passing ability, and resistance to segregation [2]. These tests are labour-intensive, time-consuming and therefore expensive. Moreover, observations made from tests under one set of conditions are not always unconditionally applicable to other circumstances in which dissimilar materials and mix proportions than the test mixes may be used. Thus, new tests are required in such circumstances. Repeated experimental tests can be avoided by performing a cost-effective computational simulation to save cost, time, effort and materials [3]. It can also provide a thorough understanding of the SCC flow behaviour, particularly in complex formworks, which is essential to achieving high quality finish. Indeed, modelling has brought insight into the significance of the rheology as a tool for the optimisation of mix composition and the processing techniques to fulfil the levels of engineering properties required for the intended civil engineering applications [4].

The flow-ability, passing/filling ability and stability can be considered as the distinguishing requirements of fresh SCC. These requirements are not common to conventional vibrated

concrete and, therefore, are handled through special tests. One of these tests is the V-funnel test, which is designed to reveal the filling ability and segregation resistance of an SCC mix; shorter discharge time ($t_{v\text{-}funnel}$) indicates greater filling ability [5]. The V-shape restricts the flow, and prolonged discharge times may provide an indication of blocking.

In this paper, the flow of SCC through a V-funnel is simulated from the moment the gate is opened until the time when the light is first seen in the bottom opening through observation from the top.The choice of the right simulation strategy is an important issue, and several approaches have been tried to simulate the flow [6–8]. Of these approaches, the smooth particle hydrodynamics (SPH) is particularly suitable because it permits to treat SCC as a homogeneous viscous fluid yet allows particles of different sizes to be tracked during the flow. This approach can also assist in proportioning SCC mixes, thus improving on the traditional trial and error SCC mix design [9–11]. It has already been successfully used to simulate the flow and to monitor the movement of large aggregates and/or short steel fibres of SCC in the slump cone flow, L-box and J-ring tests [12–15]. The SPH approach also provides a useful tool for an accurate estimation of the yield stress (τ_y) of SCC mixes in an inverse manner from the flow spread [16]. This is particularly relevant to the characterisation of an SCC mix because the measurement of τ_y and that of the plastic viscosity (η) by rheometers is inconsistent and fraught with inaccuracies. For one and the same SCC mix different rheometers are known to give vastly different values of τ_y and η [17,18]. The published results are therefore highly unreliable.

The aim of this paper is to extend the SPH approach to simulating the flow of SCC through the V-funnel. The capabilities of the SPH methodology will be validated on several SCC mixes differing by their cube compressive strength and plastic viscosity. The simulated discharge times will be compared with those recorded in the laboratory on the same mixes. As the SPH allows the distribution of large coarse aggregates embedded in the homogeneous mixes to be

tracked it is possible to check whether or not they are homogeneously distributed during the flow and after the flow has stopped. For this, the distribution of large coarse aggregates in the mix will be examined along three zones of the V-funnel at different times during the flow and along three portions of the collecting container at the outlet of the funnel after the flow has stopped. Along all these cut regions the distribution should be nearly the same if the large aggregates are indeed uniformly distributed.

The successful simulation of the flow of SCC through a V-funnel has the added advantage that the same methodology can be used to simulate the flow from a feed hopper into a mould which is the common method for the casting of SCC structural elements in a precast factory. There is a further advantage in simulating the flow in a V-funnel. As mentioned above, a well-proportioned SCC mix must provide a sufficient level of viscosity and prevent segregation of coarser aggregates in the pouring process. The coarser aggregates must remain homogeneously distributed in both the vertical and horizontal directions to ensure uniform filling of deep sections, such as walls and columns. In fact, the ASTM C1610/C1610M [19] standard procedure for assessing the segregation resistance of an SCC mix requires that the masses (i.e. concentration) of coarse aggregates in two selected washed concrete portions of equal volume of a cylindrical container retained on a 4.75 mm (No. 4) sieve be the same. The procedure can be used on the SCC mix collected in a cylindrical container after it has been discharged fully from the V-funnel. Thus the V-funnel test is useful not only for assessing the flowability of an SCC mix, but also its segregation resistance.

2. Test SCC mixes used for simulation

For the purposes of comparison with SPH simulations, a range of SCC mixes were designed (for mix proportions see Table 1) according to the rational mix design procedure described in [20] and tested to satisfy the self-compactibility criteria i.e. the filling ability, passing ability,

and resistance to segregation (i.e. stability) using the slump cone, V-funnel, J-ring, and L-box tests according to the requirements of British Standards [5,21](see Table 2). It should be stressed that the simulation technique is generic and not restricted to the six test mixes.

Table 1. Mix constituents (kg/m^3) of SCC mixes

Constituents		SCC mix designation by compressive strength (MPa)					
		30	40	50	60	70	80
cm [a]	Cement	240	262.5	281.25	315	345	367.5
	ggbs	80	87.5	93.75	105	115	122.5
Limestone powder [b]		156	147	139	125	123	125
Water		201.6	199.5	198.8	197.5	184.0	171.5
Super-plasticiser		1.6	1.7	2.1	2.4	2.8	3.0
Fine aggregate [c]		788	775	760	735	735	735
Coarse aggregate [d]		840	840	840	840	840	840

a: Cementitious materials. (Cement type II/B-V 32.5R)

b: Limestone powder ≤ 125 μm.

c: Fine aggregate ≤ 2 mm.

d: Coarse aggregate ≤ 20 mm (crushed limestone).

Table 2. Self-compactibility criteria

Test		SCC mix designation by cube compressive strength (MPa)					
		30	40	50	60	70	80
Slump flow	Spread, mm	665	675	680	650	750	750
	t_{500}, s	0.88	1.13	1.23	1.32	1.45	2.06
V-funnel	$t_{v\text{-}funnel}$, s	2.45	3.10	3.60	4.05	4.95	6.10
J-ring	Spread, mm	635	670	650	645	720	730
	t_{500j}, s	1.04	1.20	1.40	1.43	2.09	2.70
L-box	t_{200}, s	0.57	0.63	0.73	0.81	1.15	1.62
	t_{400}, s	1.11	1.23	1.37	1.72	2.49	3.20
	H_2/H_1	0.84	0.91	0.93	0.84	0.95	0.90

3. SPH Modelling of SCC flow

Since SCC flow through the V-funnel test is a gravitational flow with large deformations, the three-dimensional smooth particle hydrodynamic (SPH) mesh-less numerical approach is preferred to solve the governing equations of SCC flow [3]. The essential equations solved in the SPH are the incompressible mass and momentum conservation equations, together with the constitutive relation of the viscous fluid [3]. The fluid continuum is discretized into a limited number of particles (N), which possess all the individual material properties; this feature is the principal strength of the SPH approach. The field variables and their gradients are approximately considered and interpolated from values at a discrete set of particles in a domain of influence (Fig. 1). The partial differential equations of motion of continuum fluid dynamics are transformed into integral equations over the particles by using an interpolation function. This interpolation is conducted by ‘‘kernel estimate’’ of the field variable at any particle. All randomly generated particles, which represent the paste and the large aggregates, form a homogeneous mass with the same properties as the continuum except their assigned volumes.

In the present work, the cubic spline kernel function is used for interpolation. The viscous SCC fluid is described by a Bingham-type constitutive relation which contains two material properties, yield stress (τ_y) and plastic viscosity (η). From a computational perspective, it is expedient to approximate the bi-linear Bingham constitutive model with a kink at zero shear rate $\dot{\gamma}= 0$ by a continuous function (see, e.g. [13]). The constitutive model is coupled with the isothermal Lagrangian mass and momentum conservation equations. A projection method based on the simple predictor-corrector time stepping scheme is used to track the Lagrangian non-Newtonian flow [22,23], and the incompressibility condition is met exactly through a pressure Poisson equation. The time step is chosen based on the relevant stability conditions.

In the present problem, the time step is primarily controlled by the effective plastic viscosity and the chosen (cubic spline) kernel function.

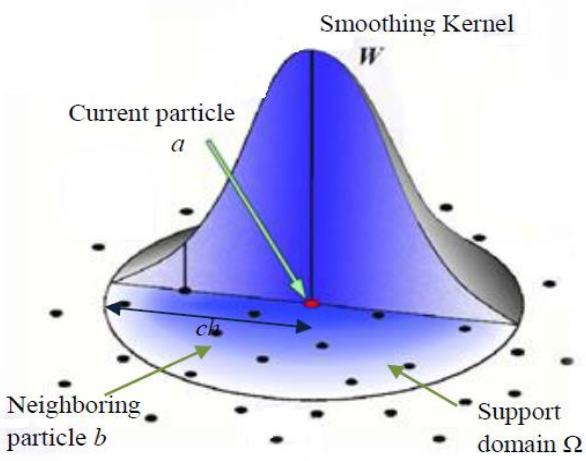

Fig. 1. Particle approximations using neighbouring particles within the support domain of the smoothing kernel *W* for particle a [3]

4. Initial configuration and boundary conditions

To solve the mass and momentum conservation equations, it is necessary to impose appropriate initial boundary conditions. Three sorts of boundary conditions have been taken into consideration in modelling the flow in the V-funnel: zero pressure condition on the free surface (*P=0*), Dirichlet boundary condition on the normal component of the particle velocity at the V-funnel walls ($v_n = 0$), and Neumann conditions on the pressure gradient ($\partial P/\partial n = 0$) (zero pressure gradient is used only for solving the second-order Poisson equation to find the pressure) as illustrated in Fig. 2, where the dimensions of the V-funnel apparatus are also given [5]. The boundary conditions are the same along all the V-funnel and rectangular outlet sidewalls. Four arrays of rigid dummy particles are placed outside the walls of the V-funnel to implement the wall boundary conditions with space r_0 between the arrays, where r_0 is the initial particle spacing. For clarity of presentation, the dummy particles are shown in two dimensions

in Fig. 2. In order to calculate the frictional force on the sides of the V-funnel resisting the free gravitational flow, the kinematic coefficient of friction (c_f) between the V-funnel walls and the SCC mix acting on the tangential component of the particle velocity has to be known. This is the only free parameter in the simulations. It has been established by matching the experimental and simulated discharge times of one test mix. The coefficient so obtained is then used for all the remaining five SCC mixes.

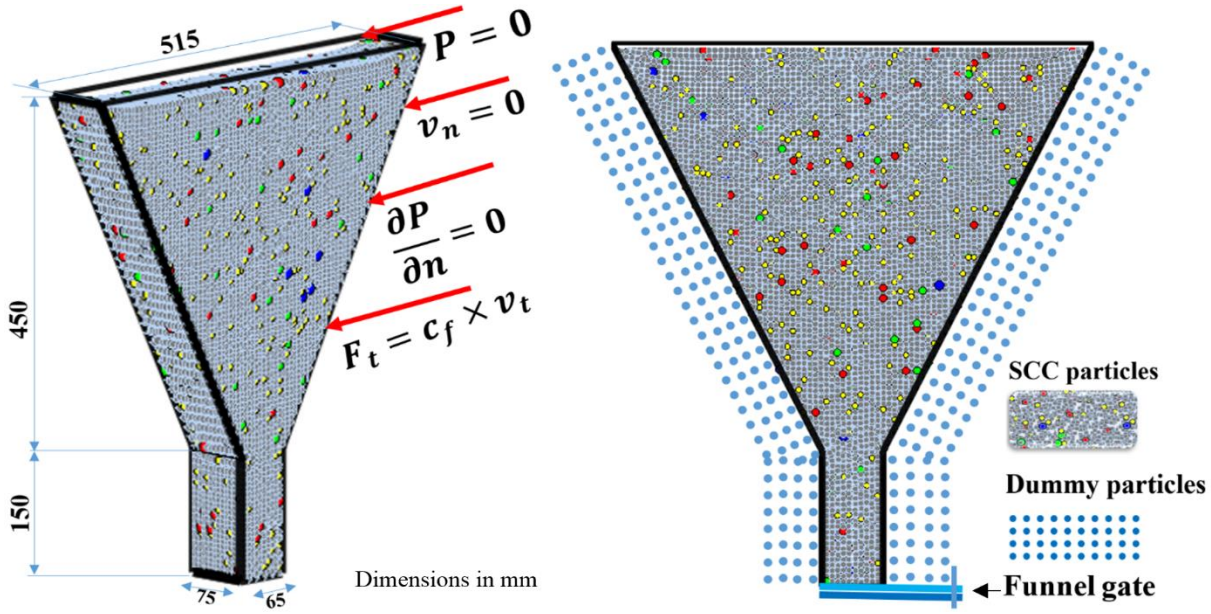

Fig. 2. Geometry and boundary conditions of the V-funnel apparatus

5. Treatment of large aggregates

An essential requirement of an SCC mix is that heavier aggregate particles do not segregate from the paste but remain homogeneously distributed during the flow. The number of particles used to represent the volume of the V-funnel contents sets a lower limit on the volume element that can be distinguished from the homogeneous mass, i.e. the resolution of the modelling technique. In the numerical implementation, a total of 53,846 particles has been used to represent the volume of the SCC mix in the funnel ($\approx 10.5 \times 10^6$ mm^3) giving a resolution of 195.35 mm^3, if all particles have the same density as the homogeneous viscous continuum. The

resolution will be somewhat different if the particles have various densities. Thus, in all mixes, the volume of large aggregates that can be distinguished from the homogeneous mass must exceed this minimum value. That is why only the aggregates of size approximately 8 mm can be distinguished in the homogeneous mass. To track the positions and velocity vectors of coarse aggregates of different representative sizes, the particles are represented by distinct colours and generated randomly, as shown in Fig. 3. It should be emphasised however that the homogeneous mass characterised by its yield stress (τ_y) and plastic viscosity (η) is formed by all particles, including the large aggregates, and the viscous mortar.

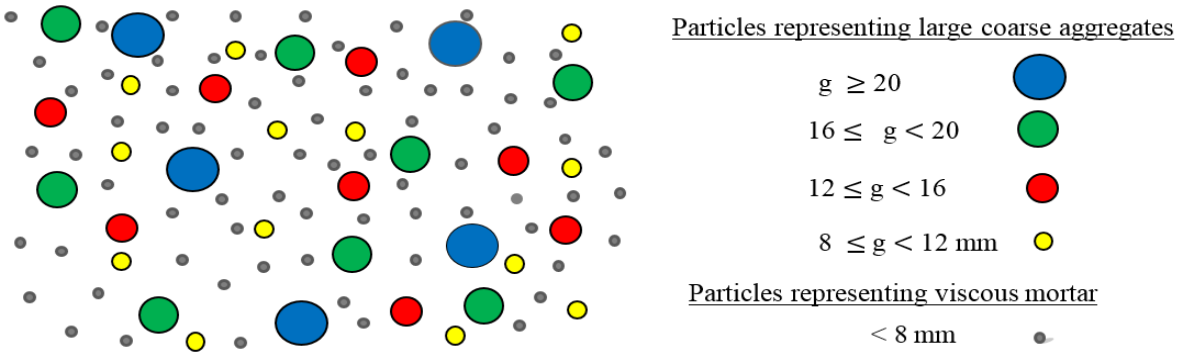

Fig. 3. Schematic sketch of particle representation when modelling large aggregate distribution [24]

The following steps were also taken during the numerical simulations:

- All particles representing the SCC mix were randomly generated;
- Particles representing the mortar and the large aggregates form a homogeneous mass and have the same continuum properties except for their assigned volumes (Table 3);
- The masses of the SPH particles representing the large aggregate particles in the SCC mix were determined based on their respective volume fractions in the SCC mix;

- Particles representing the large aggregates according to their assigned volumes were tagged and colour coded (as shown above in Fig. 3) throughout the simulation process to monitor their positions and velocity vectors.

Table 3. Volume fractions of particles of SCC mix in the 3D simulation of V-funnel

		Particle size range mm	Representative particle diameter mm	Density kg/m^3	Volume fraction %	3D V-funnel test	
						Number of particles	Assigned volume per particle mm^3
Particles	≥8 mm	g ≥ 20	20	2800	1.42	36	4960.2
		16 ≤ g <20	18	2800	8.02	276	3616.0
		12 ≤ g < 16	14	2800	4.62	338	1701.3
		8 ≤ g < 12	10	2800	8.80	1769	620.0
	<8 mm	g < 8	8	2237	77.13	51427	149.2
	Total	-	-	2365.5	100	53846	-

6. Numerical results

In the three-dimensional numerical simulation of the flow through the V-funnel, each SCC mix has been represented by a limited number of particles (53,846) to investigate its flow characteristics and compare with the corresponding experimental results. This number of particles has been chosen to provide adequate accuracy in a reasonable time. The simulation also reveals the distribution of the large components in SCC mixes (coarse aggregate size (g) ≥8 mm) so that it can be ascertained whether these heavier aggregates remain homogeneously

distributed in the viscous mix during the flow. As mentioned above, the measurement of τ_y and that of η by rheometers is inconsistent and fraught with inaccuracies. For one and the same SCC mix different rheometers are known to give vastly different values of τ_y and η [17,18]. Thus the published data cannot be regarded as reliable. For this reason, the plastic viscosity of all test SCC mixes was estimated following the procedure described in [25], based on the plastic viscosity of the paste (i.e. cement, ground granulated blast furnace slag (ggbs), water, super-plasticiser, and entrapped air). This procedure is based on the rheology of concentrated suspensions [26,27], and it can predict accurately in a stepwise way the plastic viscosity of the heterogeneous SCC mixes beginning with the plastic viscosity of the homogeneous paste which can be accurately measured with a viscometer. The yield stress, on the other hand, was estimated in an inverse manner from the measured time to stop (i.e. flow spread) of the SCC mixes in a flow cone test using SPH [16]. The plastic viscosities and yield stresses, as well as the densities of all test SCC mixes, are given in Table 4.

Table 4. Rheological properties and density of the test SCC mixes

	SCC mix designation by cube compressive strength (MPa)					
	30	40	50	60	70	80
Plastic viscosity, Pa s	4.85	7.11	8.13	8.58	9.80	11.02
Yield stress, Pa	175	175	178	180	180	190
Density, kg/m^3	2307.1	2313.2	2315.1	2319.9	2344.8	2365.5

The flow patterns of two representative test mixes obtained from the numerical simulation at various time steps are shown in Figs. 4 and 5. The experimental discharge times of all six mixes agree well with the simulated ones from SPH as reported in Table 5. The slight difference between the experimental and simulated discharge time ($t_{v\text{-}funnel}$) may be due to two possible reasons. Firstly, the assumption that the SCC particles are spherical in shape and secondly, the

slight time delay in opening the bottom gate. The delay is the greater the higher the pressure on the gate, i.e. the higher the density of the mix. Thus, the difference is the least in the 30 MPa mix because it is the lightest (density 2307.1 kg/m^3) and it is the largest in the 80 MPa mix because it is the heaviest (density 2365.5 kg/m^3).

It is worth stressing that the only free variable that has been altered in the simulation to get this excellent fit was the kinematic coefficient of friction between one SCC mix and the V-funnel sidewalls. The value that gave this agreement with the experimental result was equal to 0.55 N s/m. This value was held constant for all the remaining five mixes. It can be observed from the simulated flow illustrated in Figs. 4 and 5 that the larger aggregates do indeed appear to remain homogeneously distributed in the mix at various times during the flow and do not settle downwards. However, this needs detailed investigation, as will be described later.

Table 5. Experimental and simulation results by SPH of V-funnel discharge time

		SCC mix designation by compressive strength (MPa)					
		30	40	50	60	70	80
Discharge time ($t_{v\text{-}funnel}$), s	Experimental result	2.45	3.10	3.60	4.05	4.95	6.10
	Simulation result	2.35	2.95	3.40	3.80	4.55	5.60

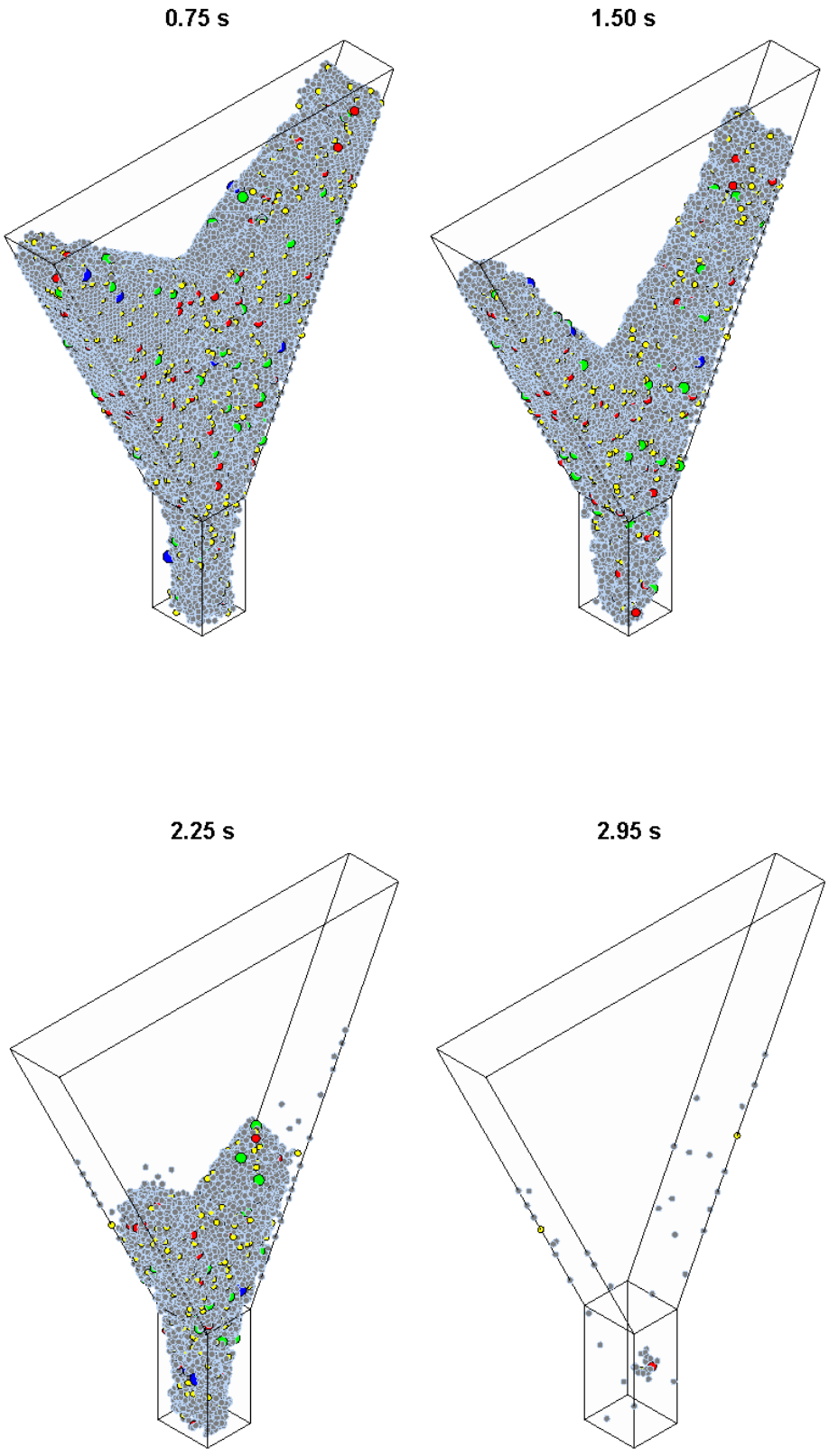

Fig. 4. Simulated flow patterns of 40 MPa mix at different time steps

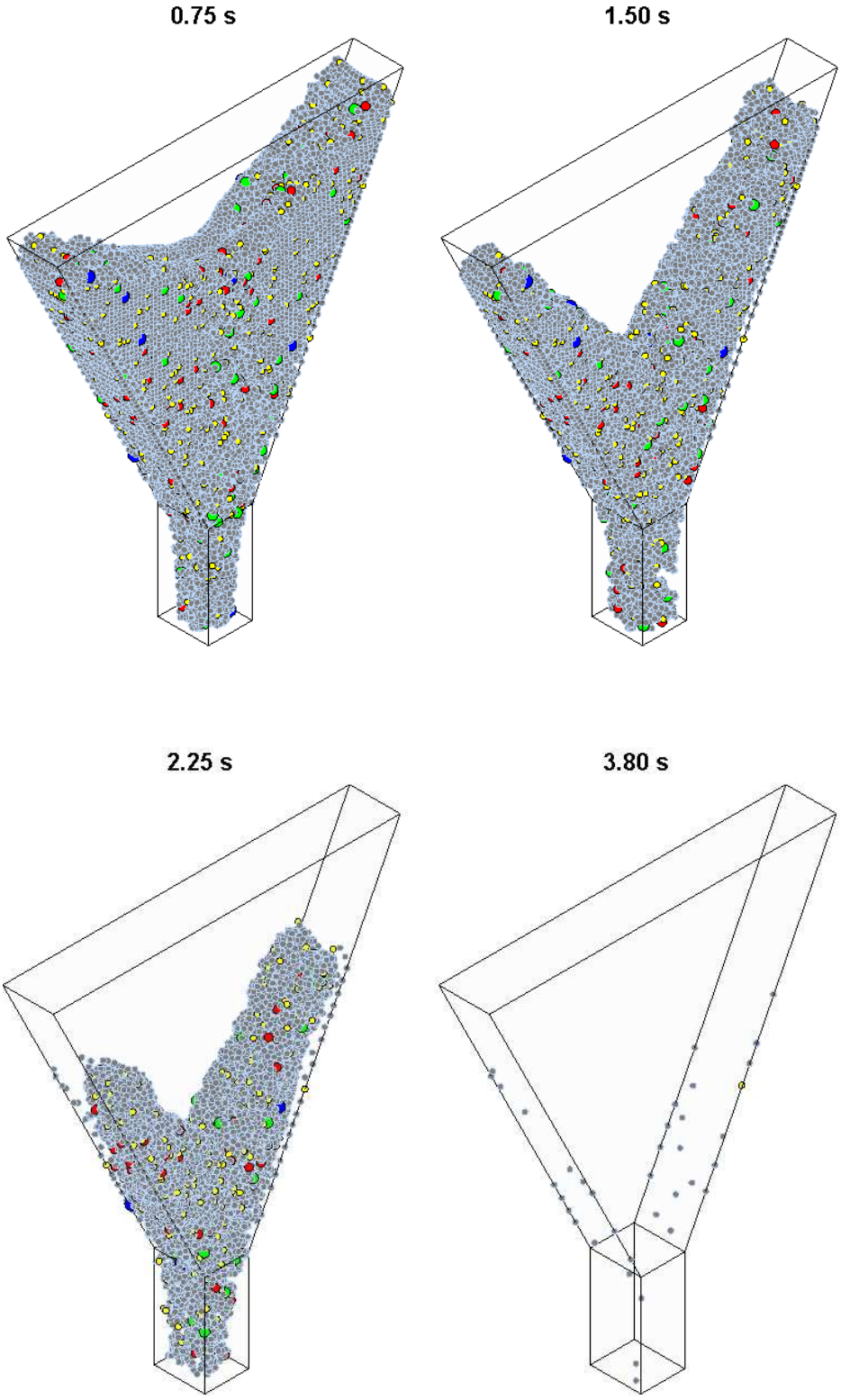

Fig. 5. Simulated flow patterns of 60 MPa mix at different time steps

The three-dimensional plots in Figs. 4 and 5 give an exaggerated and somewhat misleading impression that the particles have separated far away from the walls of the rectangular outlet. To get an accurate picture, the front and side views of the flow of the two mixes of Figs. 4 and

5 are shown in Figs. 6 and 7 at the beginning of flow and at a later time. It is clear that the particles do indeed lose contact with the sides of the rectangular outlet. This is because the flow now is essentially gravitational with the velocity vectors of the particles near the sides being primarily vertical, so that the Dirichlet boundary condition on the normal component of the particle velocity ($v_n = 0$, Fig. 2) is identically satisfied. This is confirmed by the velocity vector field of particles shown in Fig. 8. For clarity of presentation, the magnified field is shown in two dimensions.

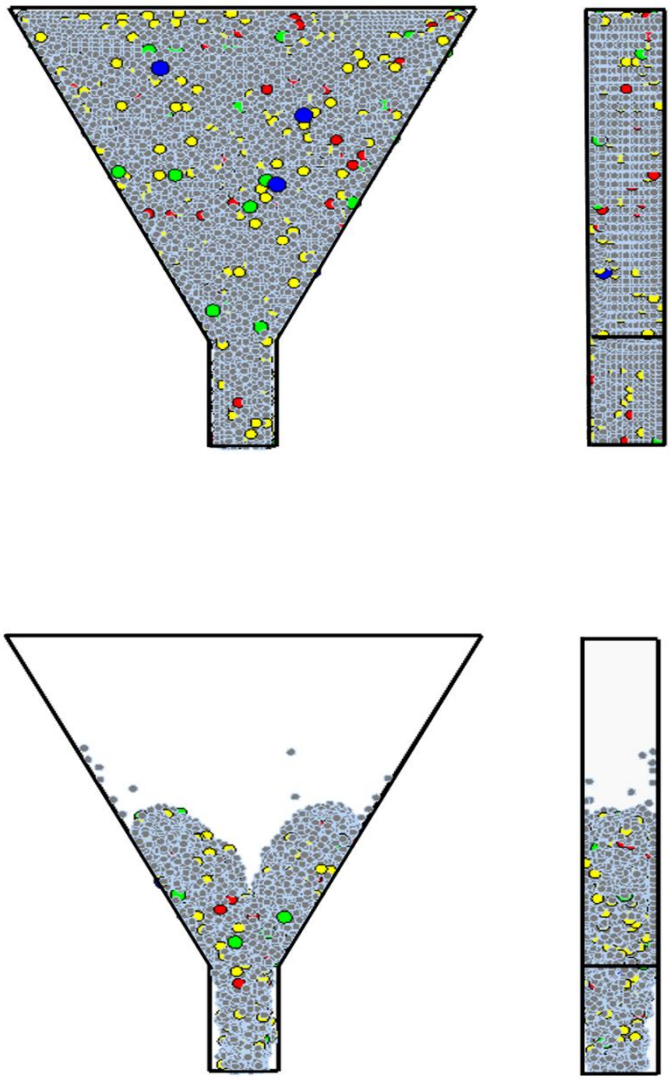

Fig. 6. Front and side views of the flow pattern of 40 MPa mix at two time steps (top: 0.01 s, bottom: 2.25 s)

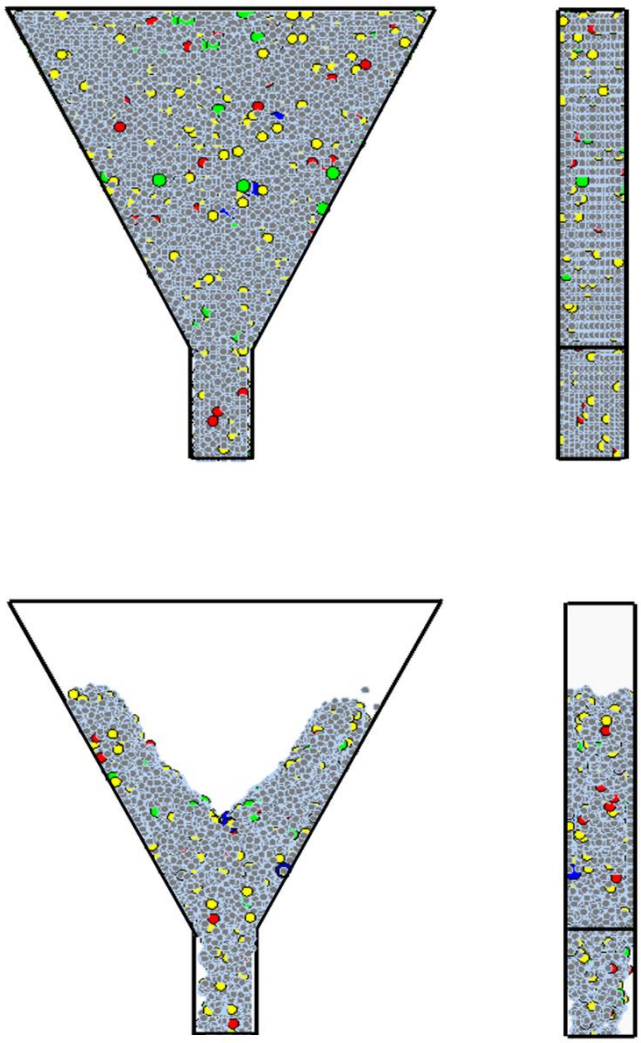

Fig. 7. Front and side views of the flow pattern of 60 MPa mix at two time steps (top: 0.01 s, bottom: 2.25 s)

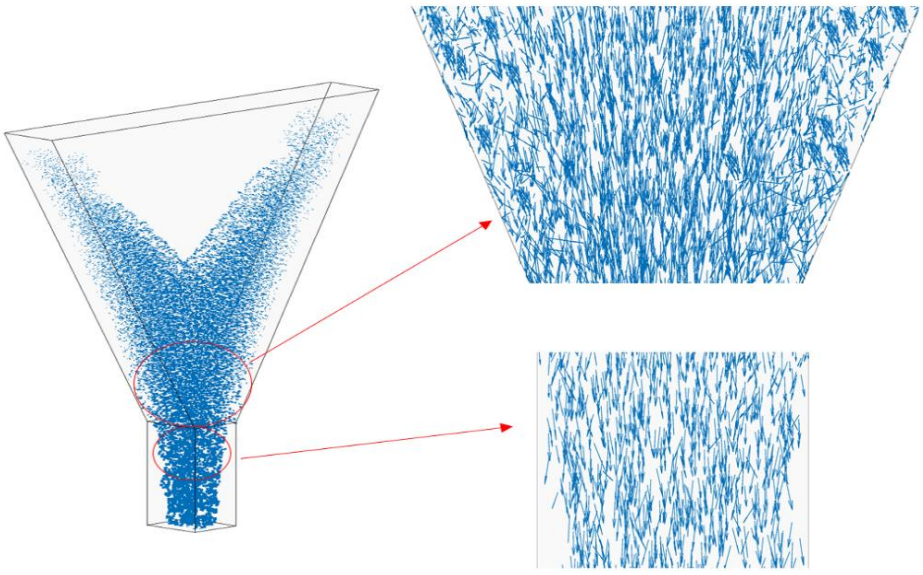

Fig. 8. Snapshot of the velocity vector field of a typical mix during the flow. The magnified 2D projection of the velocity vectors clearly shows that the dominant component of the particle velocities in the rectangular outlet is vertical.

7. Large coarse aggregate distribution

The three-dimensional SPH simulation is very useful in revealing whether heavier aggregates (aggregates ≥ 8 mm) remain homogeneously distributed in the viscous SCC mix during the flow and when it has fully discharged to the container below. For the former, the distribution of large coarse aggregates in SCC mixes will be examined by two different approaches: (i) the volume of material in the funnel and the outlet rectangular portion is divided into equal halves vertically and the distribution of large coarse aggregates examined in each half, (ii) and the volume of material in the funnel and the outlet rectangular portion is divided into three zones, not necessarily of equal volume, and the distribution of large coarse aggregates examined in each zone. The distribution of large coarse aggregates in the cylindrical container used to collect the SCC mix after it has been fully discharged from the V-funnel will be examined by dividing the container into three equal volumes. The results are discussed below.

7.1 Distribution in vertical halves

The large coarser aggregate distribution along left and right halves of the V-funnel, as shown in Fig. 9 was investigated on the 40 MPa SCC mix by performing a statistical analysis on the large coarse aggregates exposed in these halves at various time steps using the Weibull cumulative distribution function (CDF).

It can be noticed from Fig. 10 that the distributions of the large coarse aggregates of various size ranges are almost identical along the left and right halves, thus attesting to their homogeneous distribution in the mix during the flow. In addition, there is no sign of any grouping (i.e. blockage) of coarser aggregates in the narrow outlet opening.

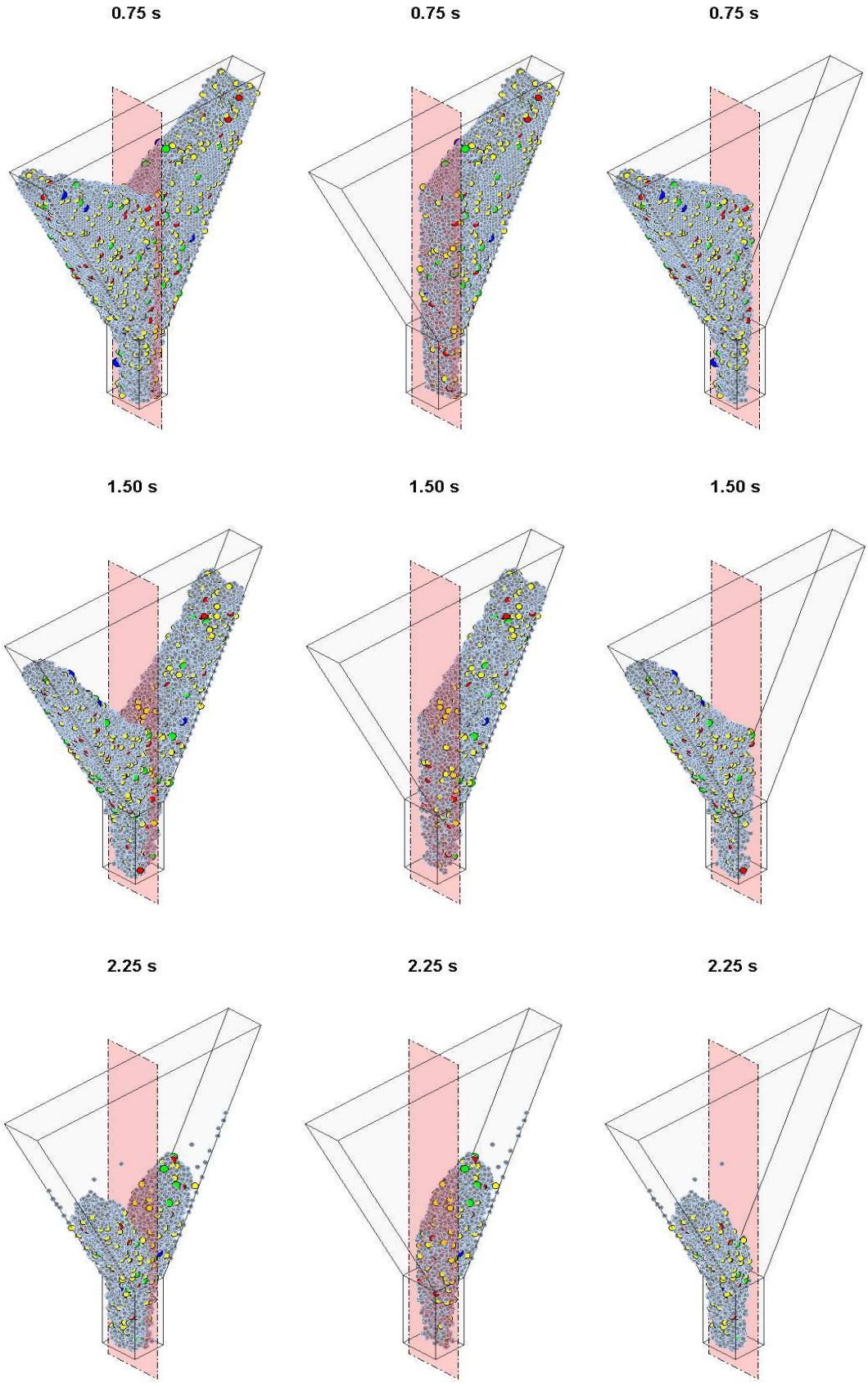

Fig. 9. The left and right halves of the V-funnel for 40 MPa Mix at various time steps (top: 0.75 s, middle: 1.50 s and bottom: 2.25 s)

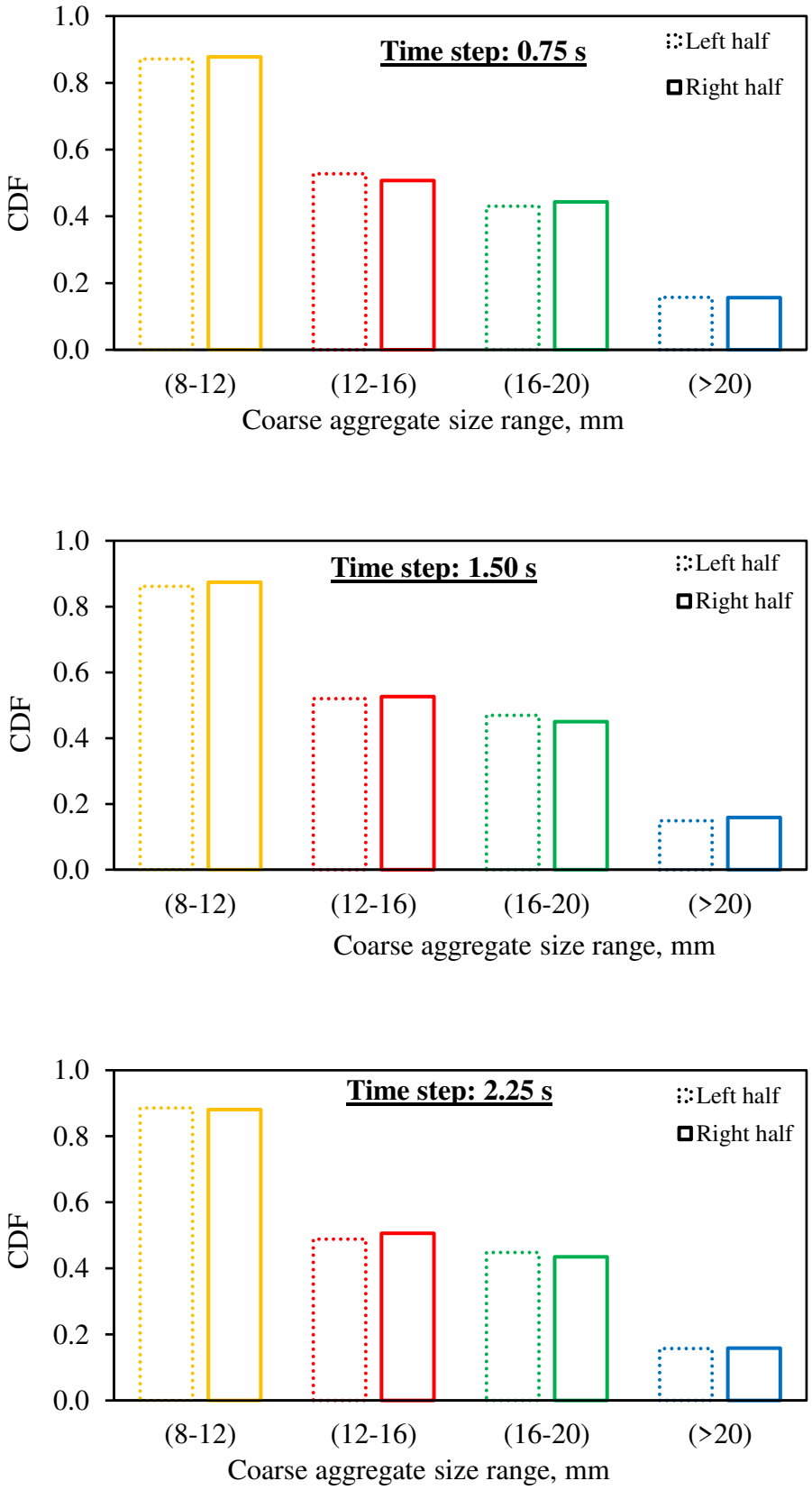

Fig. 10. Distribution of large coarse aggregates along the left and right halves of the V-funnel for Mix 40 MPa at various time steps during the flow

7.2 Distribution in three horizontal zones

In this approach, the distribution of large coarse aggregates of the 60 MPa SCC mix was examined by dividing the V-funnel into three zones horizontally : top, middle and bottom zones (as shown in Fig. 11), and counting the number of large coarse aggregate particles of each size range in the volume of material within each zone. It can be seen from the Weibull cumulative distribution function in Fig. 12 that the larger aggregates are indeed distributed almost identically in all three zones with no bias.

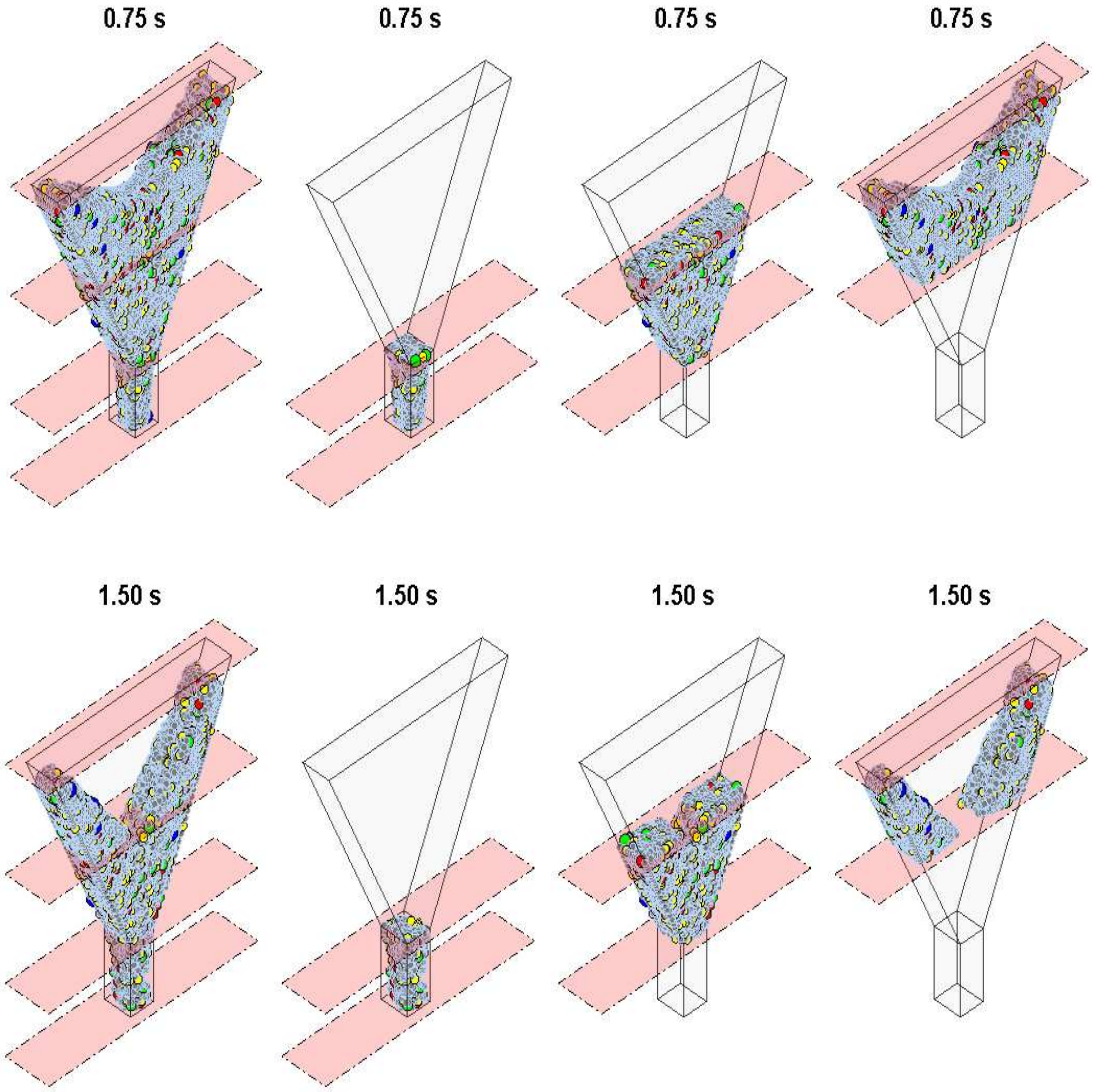

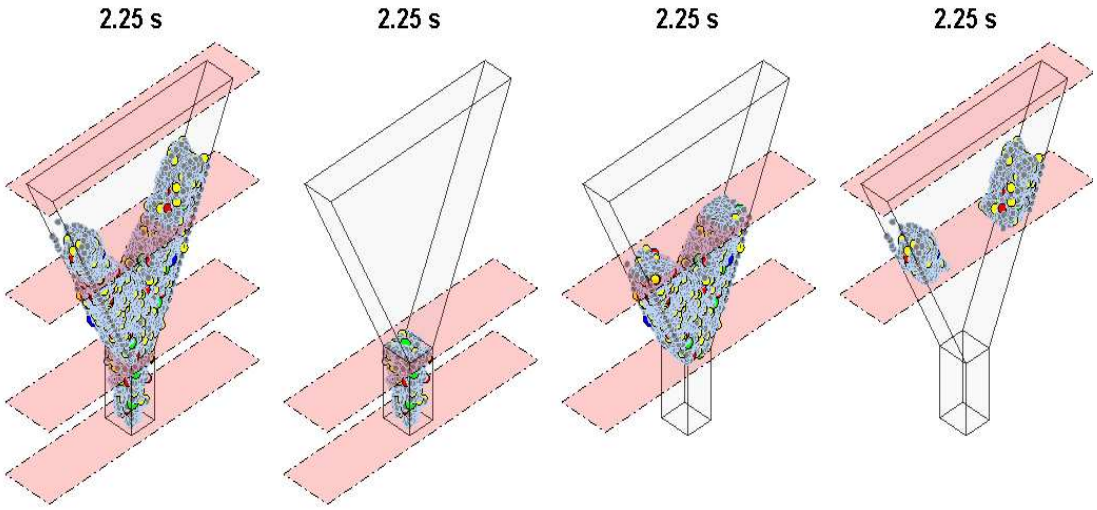

Fig. 11. The three zones of the V-funnel for 60 MPa Mix at various time steps

(from left; first: the funnel; second: bottom zone; third: middle zone, and fourth: top zone)

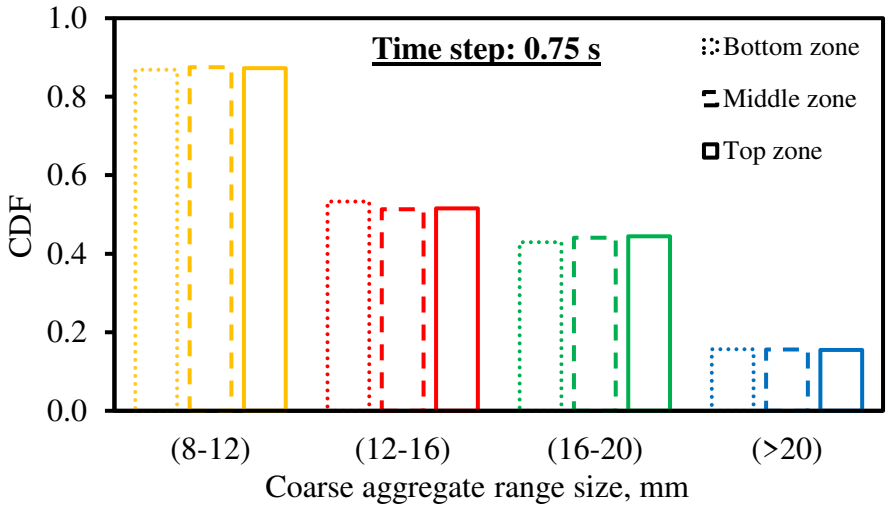

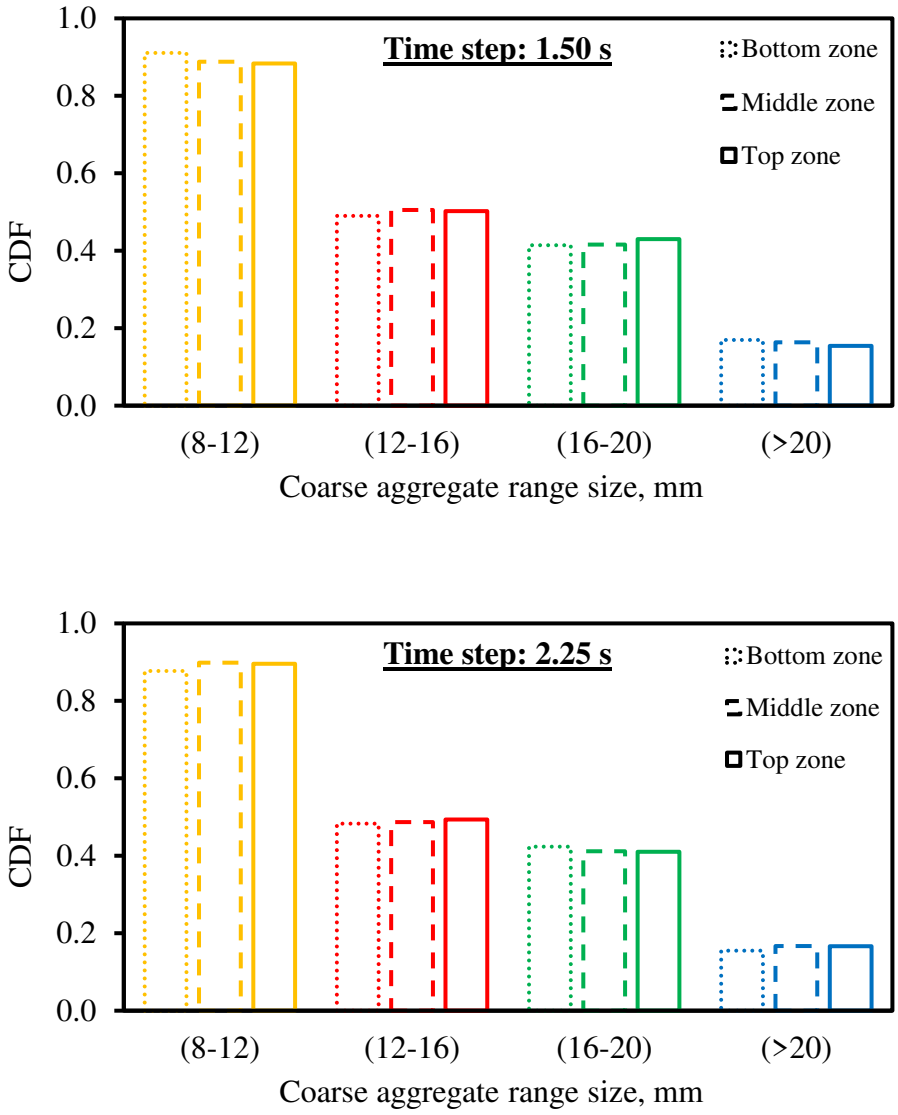

Fig. 12. Large coarse aggregate distributions in three zones of the V-funnel for 60 MPa Mix at various time steps

7.3 Large coarse aggregate distribution in the collection container

The procedure proposed in ASTM C1610/C1610M [19] to assess the segregation resistance of an SCC mix has been applied here to investigate the distribution of large coarse aggregates than their concentration on 40 MPa SCC mix after it has fully discharged into a cylindrical container from the V-funnel. The distribution has been examined in three equal portions (top, middle and bottom) of the cylindrical container beneath the V-funnel (Fig. 13). The distribution of the large coarse aggregates in each of three portions should be nearly identical to claim that there is no

segregation in the mix. Equality of total concentration (i.e. mass) of large coarse aggregates in the three portions is no guarantee that the concentration in one or more portions is not dominated by one or more large aggregate size ranges.

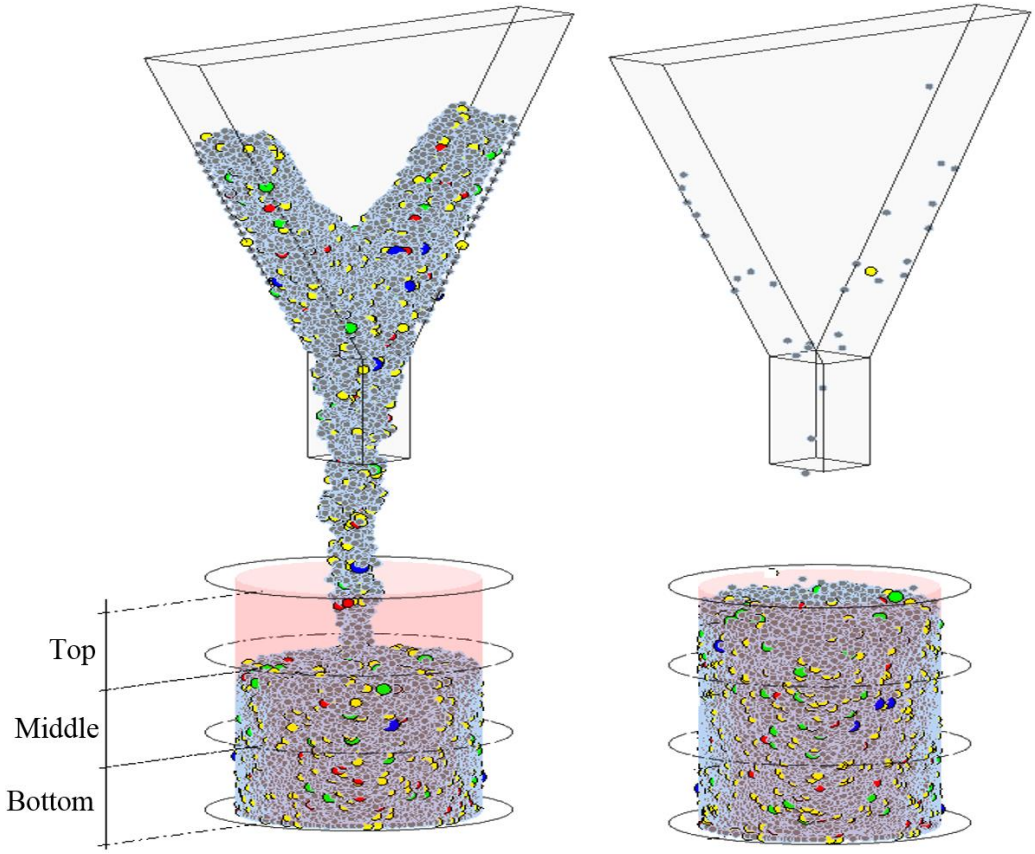

Fig. 13. Division of the cylindrical container into three equal portions to evaluate the distribution of large coarser aggregates in the 40 MPa SCC (left: during discharge from V-funnel; right: after full discharge).

The Weibull cumulative distribution function (CDF) of the different large aggregate size ranges in the three equal portions of the cylindrical collection container (Fig. 14) shows that the large aggregates do stay remarkably homogeneously distributed in the test mix without any settlement of the heavier aggregates.

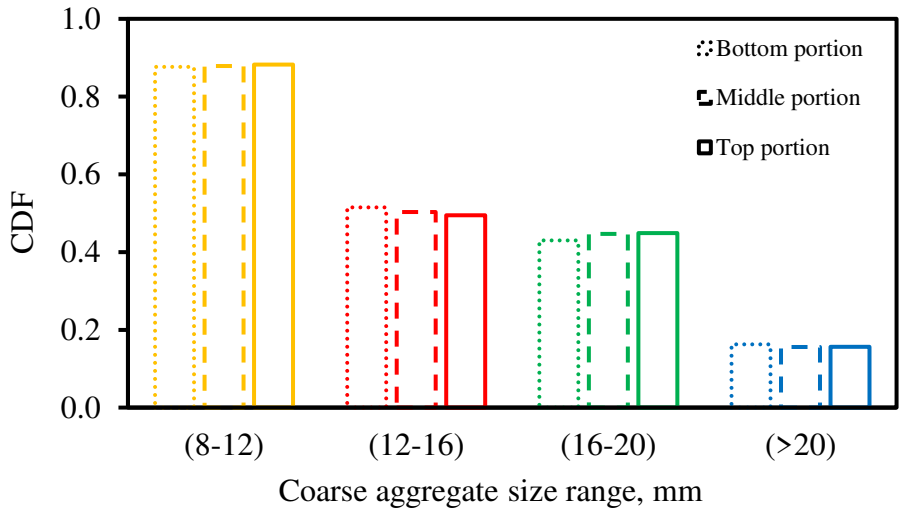

Fig. 14. Large coarse aggregate distributions in three portions of the cylindrical collector of the discharge from the V-funnel of 60 MPa Mix.

8. Remarks on simulation strategies

The flow through V-funnel has been modelled above in the real three-dimensional configuration. This takes time and effort. That is why two-dimensional approximate simulations have been reported in the past. It is unlikely that such approximate simulations will produce realistic discharge times. Moreover, two-dimensional simulations can be rather misleading because the coarse aggregate particles will appear in a single plane irrespective of their distribution. The real three-dimensional simulation shows the actual distribution of different sizes of coarse aggregate and their locations, as shown above. To compare the approximate two-dimensional simulations with the real three-dimensional ones, the two SCC mixes developed in [28] and simulated by Lagrangian smooth particle hydrodynamics (SPH) in the two-dimensional approximation of V-funnel in [29], have been simulated three-dimensionally. These mixes designated Mix-12 and Mix-20 in Table 6 contained coarse aggregates of maximum size 12 mm and 20 mm, respectively. The plastic viscosity and the yield stress have been predicted (Table 6) following the same procedure as for the test SCC mixes reported above [16,25].

Table 6. Rheological properties, density and the discharge time results from 2D and 3D simulations in comparison with the experimental test of SCC mixes in the V-funnel

		Mix-12	Mix-20
Plastic viscosity, Pa s		12.68	12.95
Yield stress, Pa		175	175
Density, kg/m^3		2296.0	2319.0
Discharge time ($t_{v\text{-}funnel}$), s	Experimental [25]	5.50	5.80
	2D simulation [26]	2.95	2.50
	3D simulation [present work]	5.05	5.30

It is evident from Table 6 that the discharge times predicted by the 2D simulation deviate markedly from the experimental values, whereas the three-dimensional simulation values are in good agreement with the experimental results. The deviation in the 2D approximation can be attributed to the smaller contact area of the mix with the side walls.

9. Conclusions

The three-dimensional Lagrangian SPH numerical scheme is able to simulate the flow of SCC mixes of varying compressive strengths through a V-funnel and to provide discharge times that agree very well with experimental results. It also provides insight into the distribution of larger aggregates during the flow and after the flow has stopped from which it is possible to assess the segregation resistance of an SCC mix.

In contrast, the two-dimensional approximation of the V-funnel is neither able to give any indication of the real distribution of large aggregates during the flow, nor is it able to predict the discharge times, because it underestimates the frictional resistance to the flow from the V-funnel sidewalls.

References

[1] H. Okamura, M. Ouchi, Self-compacting concrete, J. Adv. Concr. Technol. 1 (2003) 5–15.

[2] EFNARC Guidelines, The European guidelines for self-compacting concrete; specification, production and use, (2005) 63.

[3] G.R. Liu, M.B. Liu, Smoothed particle hydrodynamics - A meshfree particle method, World Scientific Publishing Co. Pte. Ltd, Singapore, 2003.

[4] N. Roussel, M.R. Geiker, F. Dufour, L.N. Thrane, P. Szabo, Computational modeling of concrete flow: General overview, Cem. Concr. Res. 37 (2007) 1298–1307.

[5] BS EN 12350-9, Testing fresh concrete: Self-compacting concrete-V-funnel test, (2010).

[6] J. Wu, C. Shu, An improved immersed boundary-lattice Boltzmann method for simulating three-dimensional incompressible flows, J. Comput. Phys. 229 (2010) 5022–5042.

[7] O. Švec, J. Skoček, H. Stang, M.R. Geiker, N. Roussel, Free surface flow of a suspension of rigid particles in a non-Newtonian fluid: A lattice Boltzmann approach, J. Nonnewton. Fluid Mech. 179-180 (2012) 32–42.

[8] F.P.T. Baaijens, A fictitious domain/mortar element method for fluid–structure interaction, Int. J. Numer. Methods Fluids. 35 (2001) 743–761.

[9] R. Deeb, A. Ghanbari, B.L. Karihaloo, Development of self-compacting high and ultra high performance concretes with and without steel fibres, Cem. Concr. Compos. 34 (2012) 185–190.

[10] B.L. Karihaloo, A. Ghanbari, Mix proportioning of self-compacting high and ultra high performance concretes with and without steel fibres, Mag. Concr. Res. 64 (2012) 1089–1100.

[11] R. Deeb, B.L. Karihaloo, Mix proportioning of self-compacting normal and high-strength concretes, Mag. Concr. Res. 65 (2013) 546–556.

[12] R. Deeb, S. Kulasegaram, B.L. Karihaloo, 3D modelling of the flow of self-compacting concrete with or without steel fibres. Part I: Slump flow test, Comput. Part. Mech. 1 (2014) 373–389.

[13] S. Kulasegaram, B.L. Karihaloo, A. Ghanbari, Modelling the flow of self-compacting concrete, Int. J. Numer. Anal. Methods Geomech. 35 (2011) 713–723.

[14] R. Deeb, B.L. Karihaloo, S. Kulasegaram, Reorientation of short steel fibres during the flow of self-compacting concrete mix and determination of the fibre orientation factor, Cem. Concr. Res. 56 (2014) 112–120.

[15] M.S. Abo Dhaheer, S. Kulasegaram, B.L. Karihaloo, Simulation of self-compacting concrete flow in the J-ring test using smoothed particle hydrodynamics (SPH), Cem. Concr. Res. 89 (2016) 27–34.

[16] F.F. Badry, S. Kulasegaram, B.L. Karihaloo, Estimation of the yield stress and distribution of large aggregates from slump flow test of self-compacting concrete mixes using smooth particle hydrodynamics simulation, J. Sustain. Cem. Mater. 5 (2016) 117–134.

[17] P. Banfill, D. Beaupr, F. Chapdelaine, F. de Larrard, P. Domone, L. Nachbaur, et al., Comparison of concrete rheometers: International tests at LCPC, National Institute of

Standards and Technology, Nantes, France, 2000.

[18] O.H. Wallevik, J.E. Wallevik, Rheology as a tool in concrete science: The use of rheographs and workability boxes, Cem. Concr. Res. 41 (2011) 1279–1288.

[19] ASTM C1610/C1610M, Standard test method for static segregation of self-consolidating concrete using column technique, 2011.

[20] M.S. Abo Dhaheer, M.M. Al-Rubaye, W.S. Alyhya, B.L. Karihaloo, S. Kulasegaram, Proportioning of self-compacting concrete mixes based on target plastic viscosity and compressive strength: Mix design procedure, J. Sustain. Cem. Mater. 5 (2016) 199–216.

[21] M.S. Abo Dhaheer, M.M. Al-Rubaye, W.S. Alyhya, B.L. Karihaloo, S. Kulasegaram, Proportioning of self-compacting concrete mixes based on target plastic viscosity and compressive strength: Experimental validation, J. Sustain. Cem. Mater. 5 (2016) 217–232.

[22] A.J. Chorin, Numerical solution of the Navier-Stokes equations, Math. Comput. 22 (1968) 745–762.

[23] S.J. Cummins, M. Rudman, An SPH projection method, J. Comput. Phys. 152 (1999) 584–607.

[24] R. Deeb, Flow of self-compacting concrete, PhD thesis, School of Engineering, Cardiff University, UK, 2013.

[25] A. Ghanbari, B.L. Karihaloo, Prediction of the plastic viscosity of self-compacting steel fibre reinforced concrete, Cem. Concr. Res. 39 (2009) 1209–1216.

[26] C.G. de Kruif, E.M.F. Van Iersel, A. Vrij, Russel W. B., Hard sphere colloidal

dispersions: Viscosity as a function of shear rate and volume fraction, J. Chem. Phys. 83 (1985) 4717–4725.

[27] I.M. Krieger, T.J. Dougherty, A mechanism for Non-Newtonian flow in suspensions of rigid spheres, Trans. Soc. Rheol. 3 (1959) 137–152.

[28] R. Zerbino, B. Barragán, T. Garcia, L. Agulló, R. Gettu, Workability tests and rheological parameters in self-compacting concrete, Mater. Struct. 42 (2009) 947–960.

[29] H. Lashkarbolouk, A.M. Halabian, M.R. Chamani, Simulation of concrete flow in V-funnel test and the proper range of viscosity and yield stress for SCC, Mater. Struct. 47 (2014) 1729–1743.